Non-Fickian Nonisothermal Model for Drying of Polymer Coatings

Madhu Vinjamur and Richard A. Cairncross
Dept. of Chemical Engineering, Drexel University, Philadelphia, PA 19104

As a sequel to our study on experimental measurements of trapping skinning in a poly(methyl methacrylate)/acetone coating, a mathematical model of non-Fickian diffusion that predicts trapping skinning is reported here including solvent transport due to a stress gradient that develops because of coating shrinkage. The predicted solvent concentration profile shows a sigmoidal shape and a front that moves into the coating. In the nearly constant rate period, the stress relaxes near the coating surface due to short relaxation times at high coating temperature. The stress relaxation causes negative non-Fickian flux. At higher gas flow rates, the negative non-Fickian flux causes the development of a thinner layer of low solvent concentration near the coating surface and a thicker layer of high solvent concentration inside the coating. Thus, more solvent remains in the coating dried at higher flows and trapping skinning occurs.

Introduction

Drying is one of the last and most critical steps in the production of polymer coatings such as audiotapes, videotapes, adhesives, and photographic films. Drying is accomplished in ovens by blowing hot jets of drying gas across or onto a polymer solution that is cast on a substrate. The aim of drying is to produce defect-free coatings (bubbles, cracks, and delamination are some of the defects that can appear during drying) that meet residual solvent specifications. Drying-gas velocity, temperature, and humidity are three important operating parameters in any industrial dryer. Modeling is a useful tool for determining the optimum operating conditions for producing defect-free coatings.

Several articles in the literature predict the drying behavior of polymer coatings by mathematical modeling. Okazaki et al. (1974) developed a set of equations to describe mass and heat transfer during the drying of aqueous solutions of poly(vinyl alcohol). The diffusion coefficient is a key material property controlling the drying of polymer coatings. The diffusion coefficients of water in poly(vinyl alcohol), which were used as input to the drying model, were measured with the microinterferometric method. The drying model predictions matched well with the experimental results, and, thus, showed the reliability of the proposed drying model. Many researchers now use the free-volume theory developed by Vrentas and Duda (1977) to describe the diffusion coefficient variation with concentration and temperature.

Yapel (1988) used a one-dimensional diffusion equation to describe drying, and showed that most of the solvent is removed in the initial stages of drying and that solvent remains inside the coating due to a sharp decrease in the diffusion coefficient at the coating surface due to low solvent concentrations. Vrentas and Vrentas (1994) developed a model to design a dryer that produces coating with a specified residual solvent content, and proposed a solution scheme to describe heat and mass transfer and coating shrinkage during drying. Gutoff (1994) developed an easy-to-use spreadsheet, to be used by drying practitioners, to calculate drying rates in a nearly constant-rate period and a falling-rate period. Cairncross (1994) constructed a drying model for multiple-zone drying of thin coated layers with infrared heating and showed that the model can be used to optimize (final residual solvent, maximum temperature, and so on) the drying conditions. Wagner et al. (1998) used an isothermal model to describe the drying of poly(vinyl acetate)/methanol coatings. They claim that the model can be utilized to determine drying times and also to estimate diffusion coefficients. Alsoy and Duda (1999) extended the theory of drying from binary to ternary systems, and claimed that the developed model can be used to design dryers that involve the drying of multiple solvents. Most of the drying models use Fick's law of diffusion (which states that mass transfer takes place due to

Correspondence concerning this article should be addressed to R. A. Cairncross.

concentration gradients) to describe solvent mass transport inside the coating during drying. *Non-Fickian transport*, however, occurs during the drying of some polymers, which can develop significant stress during drying and have a high shear modulus. This article describes a non-Fickian, nonisothermal drying model to investigate the drying behavior of polymer coatings.

Alfrey and coworkers (1966) recognized anomalous diffusion phenomena (which does not obey Fick's law) in polymer penetrant (solvent) systems in which the penetrant substantially swells the polymer. Thomas and Windle (1978, 1982) observed anomalous solvent transport during sorption of methanol in poly (methyl methacrylate) sheets. During anomalous solvent mass transport, the solvent mass uptake by the polymer sheet varies linearly with time instead of with an exponent of one-half, which is predicted by Fick's law of diffusion. Peterlin (1965) proposed that disentanglement of polymer chains during sorption of the solvent could account for the anomalous behavior. In another experiment, Barr-Howell and Gordon (1991) showed that anomalous transport, where the normalized solvent mass loss varied with time with an exponent lying between 0.5 and 1.0, occurs during the drying of *N*-methyl-2-pyrrolidone from solvent cast polymeric films below 175°C. In this work, we refer to all transport that cannot be described by Fick's law as non-Fickian transport. If the polymer solvent system exhibits non-Fickian behavior, then an accurate model of drying should include non-Fickian transport.

During drying of viscoelastic polymer solutions, the solvent leaves the coating surface and in-plane stress develops because of coating shrinkage. The stress gradient contributes to solvent mass transport in addition to the transport that occurs due to the solvent concentration gradient. The stress relaxes at a rate that depends on polymer mobility. At low solvent concentrations polymer mobility is drastically reduced, and the relaxation time becomes nearly infinite. The polymer, which is in a nonequilibrium state, relaxes to its final equilibrium state at a finite rate. During the relaxation process, the stress contribution to solvent mass transport decreases. Cairncross and Durning (1996) call this contribution the *nonequilibrium part of diffusion potential*, because it goes to zero as the polymer approaches its final state. Several first-principles, derivations of coupling of relaxation with diffusion have appeared in the literature (Neogi, 1983; Durning and Tabor, 1986; Carbonell and Sarti, 1990; Jou et al., 1991; Beris and Edwards, 1991; Lustig et al., 1992). We use the model derived by Durning and Tabor (1986) and Lustig et al. (1992) to describe the non-Fickian drying behavior of polymer coatings.

During the evaporation of solvent from the coating, the properties of the solution near the coating surface can be different from those of the solution deeper within the coating due to lower solvent concentrations at the surface. The development of a surface layer is referred to as skinning and is desirable in some processes such as membrane production where a thin surface layer with dense structure is needed to achieve high selectivity and flux through the membrane. In the production of polymer coatings, however, skinning is not desirable because it contributes to a lower drying rate, cracking at the surface, and bubble formation inside the coatings. Cairncross and Durning (1996) categorized three types of skinning of polymer coatings; literal, figurative, and *trapping.* *Literal skinning* occurs due to solidification of the top layer while the deeper coating is still liquid. *Figurative skinning* occurs when diffusion or internal resistance controls drying. In polymer solutions, a steep concentration gradient develops at the surface due to low diffusion coefficients, while concentration profile remains relatively flat deeper within the coating. This decreases the rate of removal of solvent from the coating and results in figurative skinning.

Trapping skinning is an anomalous drying behavior where residual solvent increases with an increase in the drying gas flow rate and temperature. Fick's law of diffusion, which states that the mass flux equals the product of the diffusion coefficient and concentration gradient, but cannot predict trapping skinning. By heuristic arguments Crank (1950, 1951) demonstrated that a fall in diffusion coefficient, $D(c)$, due to lower concentration at the surface, is compensated by an increase in the concentration gradient, dc/dx, at the surface such that the product, $D(c)(dc/dx)$, at the surface is higher at lower solvent concentration at the surface. Cairncross et al. (1994) considered steady-state diffusion flux through a thin film and showed that Fick's law of diffusion always predicts a higher flux through the surface of the coating at higher drying-gas flow rates or mass-transfer coefficients and extended the argument to transient drying of the coating. Based on these arguments, Fick's law of diffusion with a concentration-dependent diffusion coefficient cannot predict trapping skinning, and an additional mechanism must be responsible for the anomalous behavior. Glass transition, phase transformation, and reactions at the surface are some of the possible mechanisms for trapping skinning. This article shows how glass transition and non-Fickian transport can lead to trapping skinning.

Cairncross and Durning (1996) and Edwards (1998) included viscoelastic effects in the solvent mass conservation equation during drying to predict trapping skinning. These studies give a qualitative understanding because the models use piecewise constant (Edwards, 1998) or exponential forms (Cairncross and Durning, 1996) for the diffusion coefficient. Edwards (1998) showed that though instantaneous flux through the coating surface increases initially by increasing the mass-transfer coefficient, the accumulated flux (integral of instantaneous flux over time) decreases, thus trapping more solvent in the coating. Cairncross and Durning (1996) gave an indirect explanation of trapping skinning at higher drying gas temperatures. The drying model developed in this article differs from earlier ones in that it uses the Vrentas and Duda free-volume theory (1977) and its modified form (Wang et al., 2000) at low solvent concentrations to describe the diffusion coefficient. The model predicts trapping skinning and the development of a thick low concentration layer at the coating surface that cannot be predicted by Fickian diffusion. This article also seeks to give a quantitative and mechanistic understanding of trapping skinning.

Model Formulation

Figure 1 shows a typical coating that is being dried by forced convection. Heat transfer occurs from hot drying gas to the coating through both the top and the bottom coating surfaces. Evaporation occurs only from the top of the coating because the substrate is impermeable. A mathematical model

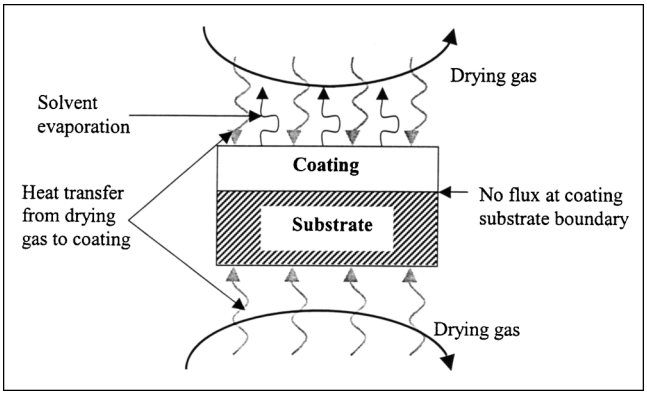

Figure 1. Heat and mass transfer during drying of a typical polymer coating cast on an impermeable substrate.

Heat transfer occurs through top and bottom surfaces of the coating, while evaporation occurs only from the top surface.

formulation of the drying process involves mass and energy conservation.

Mass conservation

The solvent continuity equation is obtained from solvent flux

$$\frac{dC}{dt} = \frac{dj}{d\xi} \tag{1}$$

Glass transition, multicomponent diffusion, and phase-transition are some of the possible explanations for trapping skinning. Romdhane et al. (2001) considered the effect of induced velocity fields and the change in partial specific volume of species for coatings that go through glass transition during drying. Initial faster drying at higher airflows reportedly results in glass formation earlier than drying at low airflows. Therefore, they state, "At higher air flows, the earlier and more abrupt decrease in solvent partial specific volumes leads to a thicker film, and, thus, higher residuals."

We utilize glass transition and stress-driven diffusion to model trapping skinning. Unlike Romdhane's model (personal communication, 2000), our model predicts a sigmoidal concentration profile, and, therefore, is phenomenologically different. Also our model predicts (discussed in the Predicted Concentration and Stress Profiles section) the formation of a thin layer of low solvent concentration near the surface and a thick inner layer of high solvent concentration. More solvent remains in a coating dried at higher airflows because the surface layer gets thinner and the inner layer gets thicker. Although we neglected the effects of volume change of mixing and induced velocity fields in the glassy state, formulating the diffusion problem in polymer coordinates has the potential to include these effects (Duda and Vrentas, 1971). We believe that inclusion of these effects will not alter the mechanism we propose in this article to predict trapping skinning.

Durning (1985) derived an equation for solvent flux using the chemical potential gradient as the driving force for solvent mass transport. Billovits and Durning (1994) utilized this equation for the flux and obtained good qualitative agreement between their experimental measurements and the theoretical predictions of the sorption behavior of polystyrene/ethyl benzene. Hence, we feel confident and justified in using the same equation for the solvent flux, j

$$j = -D\frac{\partial C}{\partial \xi} - E\frac{\partial \pi}{\partial \xi} \tag{2}$$

The solvent flux is defined with respect to the polymer motion, D is the mutual diffusion coefficient, ξ is the distance in polymer material coordinates (Billovits and Durning, 1989), C is the solvent concentration per unit volume of the polymer, $C = \rho_s/(\rho_p \hat{V}_p)$, where ρ_s is the mass concentration of the solvent and $\hat{V}_p$ is the specific volume of the polymer. π is the microscopic in-plane stress in the polymer that develops due to the coating shrinkage, and Eq. 4 describes the stress evolution during drying. The coating shrinks as it dries, and describing the mass conservation in polymer material coordinates obviates the need to write a separate equation for the coating shrinkage. E is the diffusion coefficient for the stress term in Eq. 2. Durning (1985) developed the following equation for E

$$E = D\frac{\hat{V}_s^2 M_{ws} G_o}{RT}\frac{1}{\left(1 + C\hat{V}_S\right)\left(\partial f(C)/\partial C\right)} \tag{3}$$

where $\hat{V}_s$ is the partial specific volume of the solvent, M_{WS} is the molecular weight of the solvent, G_o is the shear modulus of the pure polymer, R is the gas constant, T is coating temperature, $f(C) = \ln[a(C)]$ is the local equilibrium fugacity of the solution, and $a(C)$ is the corresponding activity of the solution. π is the microscopic stress in the polymer, which is unstressed initially, and π can be described by Maxwell's model for viscoelastic materials with a single relaxation time

$$g(C)\frac{dC}{dt} = \frac{d\pi}{dt} + \frac{\pi}{\tau_{\text{relax}}} \tag{4}$$

where $g(C)$ is the ratio of instantaneous shear modulus, $G(C)$, to the shear modulus of the pure polymer, G_o; and τ_{relax} is the relaxation time that is inversely proportional to the self-diffusion coefficient of the polymer, as shown by Eq. 11. In the Maxwell model for stress evolution, the stress relaxes exponentially to zero at constant solvent concentration. At long relaxation times, the change in stress is proportional to the change in the solvent concentration. Also, because normalized shear relaxation modulus, $g(C)$, is $O(1)$, the maximum change in the stress is equal to the maximum change in the solvent concentration.

Cairncross and Durning (1996) described and provided equations for the one initial condition and two boundary conditions that are needed to solve Eq. 1. The initial condition is the uniform solvent concentration. The boundary conditions are provided in terms of the solvent flux at the coating surface and the coating substrate. At the coating surface, the solvent flux is described by the product of a mass-transfer coefficient, K, and the difference between the solvent partial

pressure at the surface and in the bulk drying gas

$$j = KP^*_{\text{sat}}(a^+ - a^\infty) \qquad \xi = 0 \tag{5}$$

The solvent partial pressure is the solvent vapor pressure, P^*_{sat}, at the coating temperature multiplied by the activity, a. The activities of the solvent on the gas side and in the bulk gas are a^+ and a^∞, respectively. a^+ is equal to the solvent activity on the coating side, a^-, which includes the relaxation effects

$$a^+ = a^- = a(C)\exp\left(\frac{\hat{V}_s M_w G_o}{RT}\pi\right) \tag{6}$$

where $a(C)$ is the solvent activity without any relaxation effects, and it can be predicted by the Flory–Huggins theory described by Eq. 18.

At the coating substrate boundary, the solvent flux is zero because the substrate is impermeable

$$j = 0 \qquad \xi = l_p \tag{7}$$

where l_p is the dry polymer thickness.

Energy conservation

For thin polymer coatings, the heat-transfer Biot number that characterizes the ratio of resistance to heat transfer in the coating to resistance to heat transfer in the gas is low. So, it is reasonable to assume that the temperature of the coating and the substrate is uniform across the thickness. So, a lumped equation (Alsoy and Duda, 1998) describes the evolution of the coating temperature during drying

$$\left(m_1 C_{p,1} l_1 + m_2 C_{p,2} l_2 + m_3 C_{p,3} l_3\right)\left(\frac{dT_c}{dt}\right) = \left(h_{\text{top}} + h_{\text{bot}}\right)\left(T_{\text{gas}} - T_c\right) - \Delta H_v \dot{m} \tag{8}$$

where m is mass; $C_{p,1}$, $C_{p,2}$, $C_{p,3}$ are specific heats of the solvent, the polymer, and the substrate, respectively, and are assumed to be constant; l is thickness; subscripts 1, 2, and 3 stand for the solvent, the polymer, and the substrate, respectively; h_{top} and h_{bot} are the top (gas) side and the bottom (substrate) side heat-transfer coefficients; T_{gas} is the drying-gas temperature; T_c is the coating temperature; ΔH_v is the latent heat of vaporization of the solvent; and $\dot{m}$ is the solvent evaporation rate from the coating surface, and can be obtained from Eq. 5.

The coating thickness at any time is the sum of the contributions from the polymer, l_p, and the solvent, l_s. The solvent contribution to coating thickness, at any time, can be obtained from the solvent concentration profile across the coating

$$l_s = \int_0^{l_p} C\hat{V}_s d\xi \tag{9}$$

where l_s is the volume of the solvent per unit area of the coating.

Model System

We have chosen poly (methyl methacrylate)/acetone as the model system, because we have experimentally measured (Vinjamur and Cairncross, 2002) trapping skinning on this system. Vrentas et al. (1975) define a diffusion Deborah number, De, as the ratio of the characteristic relaxation time to the characteristic diffusion time

$$De = \frac{\tau_{\text{relax}}}{\tau_{\text{diffusion}}} \tag{10}$$

where τ_{relax} is the characteristic relaxation time of the polymer and can be estimated (Hassan and Durning, 1999) from the polymer self-diffusion coefficient

$$\tau_{\text{relax}} = \tau_o \frac{D_2(T_o, w_1 = 0)}{D_2(T, w_1)} \tag{11}$$

Billovits and Durning (1994) obtained a good comparison between relaxation times extracted from viscoelastic sorption data and those from using Eq. 11. Here τ_o is the relaxation time of the pure polymer at reference temperature T_o for a polymer melt, D_2, is the self-diffusion coefficient of the polymer, and w_1 is the solvent mass fraction. Employing the Vrentas and Duda free-volume theory (1977) to estimate the polymer self-diffusion coefficient, the following equation describes the relaxation time

$$\tau_{\text{relax}} = \tau_o \frac{\exp\left[-\dfrac{\gamma \hat{V}_2^*}{\hat{V}_{FH}}\right]_{T_o, w_1 = 0}}{\exp\left[-\dfrac{w_1 \hat{V}_1^* + w_2 \hat{V}_2^* \xi}{\xi \hat{V}_{FH}/\gamma}\right]_{T, w_1}} \tag{12}$$

where γ is an overlap factor, w_1 and w_2 are mass fractions of the solvent and the polymer, respectively; $\hat{V}_1^*$ and $\hat{V}_2^*$ are the specific hole free volumes of the solvent and the polymer, respectively, required for a diffusion jump; and ξ is the ratio of the molar volume of the solvent to that of the polymer-jumping unit. The hole free volume is

$$\frac{\hat{V}_{FH}}{\gamma} = \frac{K_{11}}{\gamma} w_1\left(K_{21} - T_{g1} + T\right) + \frac{K_{12}}{\gamma} w_2\left(K_{22} - T_{g2} + T\right) \tag{13}$$

where K_{11}/γ and $K_{21} - T_{g1}$ are the solvent free volume parameters and K_{12}/γ and $K_{22} - T_{g2}$ are the polymer free volume parameters (Vrentas and Duda, 1977). The numerator of Eq. 12 is evaluated at a reference temperature for pure polymer, and the denominator is computed at any temperature and solvent concentration.

The characteristic diffusion time is

$$\tau_{\text{diffusion}} = \frac{L^2}{D_M} \tag{14}$$

where L is dry polymer thickness and D_M is the mutual dif-

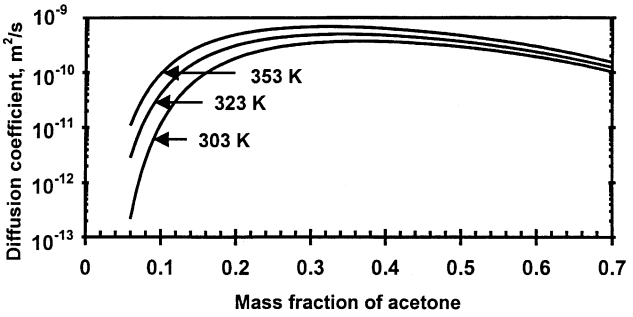

(a)

Figure 2a. Mutual diffusion coefficient of poly(methyl methacrylate)/acetone system at three different temperatures, estimated by Vrentas and Duda's (1977) free-volume theory.

Mutual diffusion coefficient is a strong function of acetone concentration and temperature.

fusion coefficient (Vrentas and Duda, 1977)

$$D_M = D_o(1-\Phi_1)^2(1-2\chi\Phi_1)\exp\left(-\frac{E_{\text{act}}}{RT}\right) \times \exp\left[-\frac{w_1\hat{V}_1^* + w_2\hat{V}_2^*\xi}{\hat{V}_{FH}/\gamma}\right] \quad (15)$$

The mutual diffusion coefficient, D_M, is estimated in the lab coordinates, unlike the one used in Eq. 2, which is evaluated in the polymer material coordinates: $D = D_M(\rho_p\hat{V}_p)^2$, where D_o is the preexponential factor, Φ_1 is the volume fraction of the solvent, χ is polymer solvent interaction parameter that can be determined from the Flory–Huggins theory (Flory, 1953), E_{act} is the activation energy, and T is the temperature.

Figures 2a and 2b show the mutual diffusion coefficient and the relaxation times predicted by Eqs. 15 and 12, respectively. Figure 2a shows that the mutual diffusion coefficient is a strong function of temperature and acetone concentration. Figure 2b shows that the relaxation times are very short at higher mass fractions of acetone and increase drastically at lower mass fractions of acetone because of a lower self-diffusion coefficient of the polymer. *De* can be $O(1)$ at higher diffusion coefficients and shorter relaxation times.

De (Vrentas et al., 1975) characterizes relative rates of shrinkage and relaxation, and, hence, whether stress gradients can contribute to the solvent mass transport. When *De* is $O(1)$, then the contribution of stress gradients to the solvent mass transport may become significant, if E is high. At very low *De*, the solvent mass transport is mainly due to concentration gradients.

Table 1 lists all the parameters needed to compute *De* for poly(methylo methacrylate)/acetone (PMMA/Ac). Figure 3 shows *De* for PMMA/Ac at three different temperatures for a 100-micron-thick dry polymer. During drying, *De* is initially very low because relaxation time is very low at high acteone concentration. Later as acetone leaves the coating surface, *De* becomes $O(1)$ at low acetone mass fractions, shown in Figure 3, and *non-Fickian* diffusion can become significant.

Table 1. Solvent and Polymer Parameters to Estimate Diffusion Deborah Number (*De*)

Solvent Parameters	Acetone	Polymer Parameters	Poly(methyl methacrylate)
D_o (m²/s)	3.6×10^{-8}	K_{21}/γ (m³/kg/K)	3.05×10^{-7}
E_{act} (J)	0.0	$K_{22}-T_{g2}$ (K)	−301
K_{11}/γ (m³/kg/K)	1.86×10^{-6}	V_2^* (m³)	7.88×10^{-7}
$K_{21}-T_{g1}$ (K)	−53.33	τ_o (s)	140
$\hat{V}_1^*$ (m³)	9.43×10^{-7}		
χ	0.4		
ξ	0.375		

Model Parameters

We use Eq. 15 to estimate the mutual diffusion coefficient in a polymer above glass transition temperature, T_g, in the lab coordinates and convert it to polymer coordinates, as de-

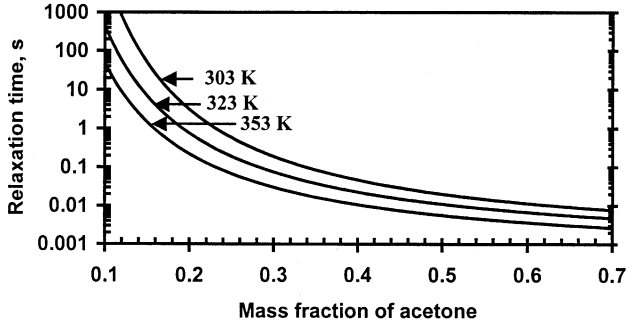

(b)

Figure 2b. Relaxation time of poly(methyl methacrylate)/acetone system at three different temperatures.

Relaxation time is inversely proportional to self-diffusion coefficient of the polymer.

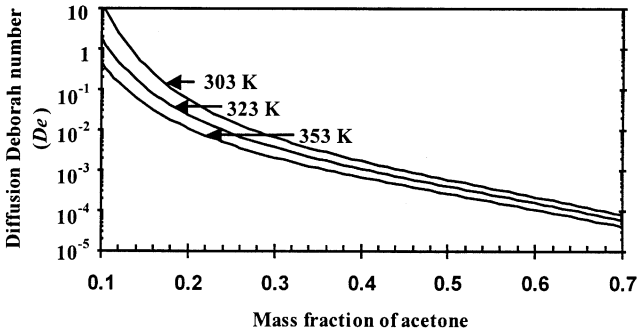

Figure 3. Diffusion Deborah number (*D/e*) for poly (methyl methacrylate)/acetone system at three different temperatures for a 100-micron dry-film thickness.

Non-Fickian diffusion due to stress gradients occurs when *De* is $O(1)$.

scribed in the model formulation. Below the glass transition Wang et al. (2000) propose a modification to the hole free volume

$$\frac{\hat{V}_{FH}}{\gamma} = w_1 \frac{K_{11}}{\gamma}\left(K_{21} - T_{g1} + T\right) + w_2 \frac{K_{12}}{\gamma}\left(K_{22} - T_{g2} + T_{gm}\right) \tag{16}$$

where T_{gm} is the glass transition temperature of the solvent polymer mixture

$$T_{gm} = \frac{x_1 \Delta C_{p1} T_{g1} + x_2 \Delta C_{p2} T_{g2}}{x_1 \Delta C_{p1} + x_2 \Delta C_{p2}} \tag{17}$$

where x_i represents the mole fraction defined on the basis of repeat unit of the polymer; ΔC_{pi} is the incremental change in the heat capacity; T_{gi} is the glass transition temperature of the pure component; and subscripts 1 and 2 denote the solvent and the polymer, respectively. Wang et al. (2000) report values of ΔC_{p2} and T_{g2} for PMMA. We used a model derived by Chow (1980) to find the reduction in the glass transition of PMMA due to acetone and then used Eq. 17 to regress for ΔC_{p1} and T_{g1}. The diffusion coefficient that characterizes the solvent transport due to stress gradients, E, can be estimated from the shear relaxation modulus of pure polymer G_o, which is obtained from Ferry (1980), and the activity of the solvent that can be predicted from the Flory–Huggins theory

$$a = \phi_1 \exp\left(\phi_2 - \chi \phi_2^2\right) \tag{18}$$

where ϕ_1 and ϕ_2 are volume fractions of the solvent and the polymer, respectively, and χ is solvent polymer interaction parameter. The vapor pressure of acetone is calculated from the Antoine equation

$$\log_{10}(P_{\text{sat}}) = A - \frac{B}{T + C} \tag{19}$$

where A, B, and C are Antoine constants. Relaxation time, τ_{relax}, is obtained from Eq. 12. Hong (1995) provides free volume theory parameters, and Fuchs et al. (1996) report terminal relaxation times for PMMA for different molecular weights. Heat-transfer coefficients that are typical of industrial dryers are chosen and the Chilton–Colburn analogy is used to estimate mass-transfer coefficients from corresponding heat-transfer coefficients. Tables 1 and 2 list all parameters required for solving the model for PMMA/acetone solutions.

The model parameters listed in Tables 1 and 2 are our best estimates based on the available literature. Nevertheless, there is still significant uncertainty in several of the parameters. The reported values for the parameters D_o, $K_{22} - T_{g2}$, K_{12}/γ, and ξ in the expression for the mutual diffusion coefficient are usually not accurate and can be estimated from drying experiments. Price et al. (1997) regress these parameters for poly(vinyl acetate)/acetone coatings from drying experiments above the glass transition temperature of the pure polymer. Chow states that the model to compute the reduction in glass transition is simple and matches well with experiments. So, we believe the regressed parameters ΔC_{p1} and T_{g1} are accurate. Fuchs et al. (1996) do not report the accuracy of relaxation time. Small errors in the model parameters do not change the model results qualitatively.

Solution of Equations

Equation 1, a partial differential equation, and Eqs. 4 and 8, ordinary differential equations, are nonlinear and coupled equations subject to boundary and initial conditions. The system of equations is solved by Galerkin's method, with finite-element basis functions. The coating is divided into 40 elements, and the values of C and π are determined at three nodal points in each element. Doubling the number of elements to 80 changed the values of C and π by at the most 0.5%, but more than doubled the computation time. So, all the calculations were made with 40 elements. C and π are interpolated by quadratic functions across every element and are continuous at element boundaries (Strang and Fix, 1973; Finlayson, 1992). The values of C and π are calculated at each node at every time step.

In the Galerkin's formulation, the equations put in residual form are weighted by piecewise quadratic basis functions and integrated over the whole domain to produce a system of dif-

Table 2. Physical Properties of Solvent and Polymer and Operating Parameters for the Drying Model

Acetone Properties		Poly(methyl Methacrylate) Properties		Operating Parameters	
Specific vol. (m^3/kg)	1.22×10^{-3}	Specific vol. (m^3/kg)	8.417×10^{-4}	h_{top} (W/m^2/K)	209 and 83.6
Specific heat (cal/g/°C)	2175.68	Specific heat (J/kg/K)	1255.2	K (m/s)	1.24×10^{-4} and 4.96×10^{-5}
Latent heat of vaporization (J/kg)	5.23×10^{5}	G_o (N/m^2)	1.35×10^{9}	Drying-gas temp. (K)	353.0
ΔCp (J/kg/K)	1673.6	ΔCp (J/kg/K)	1380.72	Initial temp. (K)	298.0
Tg (K)	50	Tg (K)	381.0	Initial acetone conc. (w/w)	85%
A	7.02447				
		Substrate Properties			
B	1161.0	Specific heat (J/kg/K)	1882.8		
C	224.0	Specific vol. (m^3/kg)	7.25×10^{-4}		
		Thickness (m)	3.556×10^{-4}		

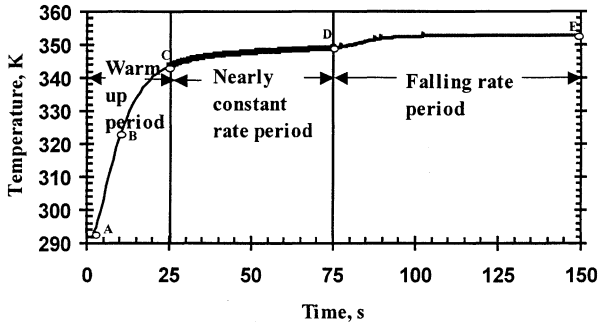

Figure 4. Temperature profile of a 100-micron dry-film thickness poly(methyl methacrylate)/acetone coating during drying at a drying-gas temperature of 353 K and a heat-transfer coefficient of 209 W/m^2/K.

Non-Fickian drying behavior is investigated in the warmup period (points *A* and *B*), in the nearly constant-rate period (points *C* and *D*), and in the falling-rate period (point *E*).

ferential equations. At each node, Gaussian integration computes the residuals. The diffusive terms of Eq. 1 are integrated by parts, and the boundary conditions are applied to the resulting boundary terms. Galerkin's method is not used for energy conservation because the temperature is uniform across the coating thickness. Earlier studies (Cairncross, 1994) have shown that a steep concentration gradient develops at the coating surface during drying. Therefore, the elements near the surface were made smaller by $p_i = ((i-1)/(n-1))^2$, where p_i is the position of the element i, and n is total number of elements.

DASSL (Petzold, 1982; Brenan et al., 1989), a nonlinear differential algebraic equation system solver, was used to solve for the set of unknowns at every time step. The vector of unknowns was solved until the root-mean-square norm of the residuals converged to 10^{-6} at every integration time step. DASSL automatically updates the time-step size to meet the error criteria. It takes about 150 s for a typical model to run on a 500-MHz desktop computer with Intel Pentium processor.

Drying Periods

The drying of the polymer coating is characterized by three drying periods, viz., warmup, nearly constant-rate, and falling-rate periods, shown in Figure 4. The coating temperature profile for the entire drying period can be used to distinguish the drying periods. The characteristic features of the non-Fickian, nonisothermal model for drying of polymeric coatings are investigated in the three drying periods.

Warmup period

The warmup period refers to the drying period where initial transients are significant. During this period, due to an imbalance between heat transfer from the drying gas to the coating and the heat consumption due to the solvent evaporation, the coating temperature can rise or fall from the initial temperature. The duration of this period is inversely proportional to the drying gas flow rate and depends on gas temperature, latent heat of vaporization of the solvent, and thermal mass of the coating–substrate system.

In the warmup period, the drying rate is high because of high diffusion coefficients at high solvent concentrations. The high drying rate results in a rapid fall in solvent concentration and concomitant development of stress near the coating surface. As the solvent concentration decreases, stress also develops inside the coating. Deeper in the coating, the stress relaxes due to short relaxation times at higher solvent concentrations. Non-Fickian transport that occurs due to stress gradients, in the direction of decreasing stress (that is, more negative stress), increases the drying rate and leads to fast drying of the polymer coating in this period.

Nearly constant-rate period

During the nearly constant-rate period, the rate of energy delivered to the coating is nearly equal to the rate of heat loss due to solvent evaporation, and, therefore, the coating temperature remains nearly constant. Strictly speaking, the coating temperature increases very slowly in this period because of a gradual decrease in drying rates due to a decrease in solvent activity at the coating surface. The duration of this period depends on the solvent activity, the latent heat of vaporization of the solvent, the mutual diffusion coefficient, and the coating thickness.

In the nearly constant-rate period, the coating temperature increases slowly and the temperature difference between the drying gas and the coating depends on the drying-gas flow rate. The difference is smaller at higher drying-gas flows and larger at lower flows. The nearly constant and higher coating temperatures at higher drying-gas flow rates, in this period, can cause stress relaxation deeper within the coating. Stress cannot relax because of the high relaxation times at low solvent concentrations close to the coating surface. Therefore, the stress decreases toward the coating surface and the *non-Fickian transport* contributes to solvent removal from the coating.

Falling-rate period

In the falling-rate period, the diffusivity at the coating surface falls due to low solvent concentrations, the drying rate decreases, and the coating temperature rises to the drying-gas temperature. During this period the drying rate is determined by the solvent transport inside the coating. In other words, internal resistance to solvent mass transport is higher than external resistance to solvent mass transfer in the gas phase. Hence, the drying-gas flow rate has no effect on the drying rate. In falling rate period, the residual solvent levels off and decreases with an increase in the drying-gas temperature.

In the falling-rate period, due to low solvent concentrations, D and E are low and relaxation times are very high. Hence, the drying rate is slow and the solvent concentration decreases very slowly. Consequently, stress increases slowly, and it cannot relax anywhere in the coating because of high relaxation times at low solvent concentrations. Due to the slow drying rate and long relaxation times, the drying behavior (concentration and stress profiles) does not change qualitatively in this period.

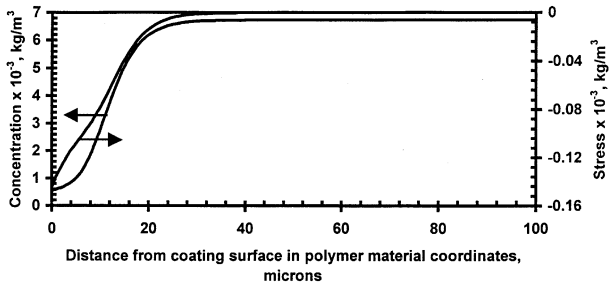

(a)

Figure 5a. Solvent concentration and stress profiles of 100-micron dry-film thickness poly(methyl methacrylate)/acetone coating in the warmup period at 1 s at point *A*.

Coating temperature is 292 K and the solvent concentration profiles is sigmoidal.

Predicted Concentration and Stress Profiles

This section probes drying behavior of PMMA/acetone solutions at high drying-gas flow rates in the three drying periods just discussed. Drying behavior is investigated just after the coating is exposed to the hot drying gas during the rise of the coating temperature in the warmup period, at the beginning and end of the nearly constant-rate period, and at a sufficiently long time after the coating temperature reaches the drying-gas temperature in the falling-rate period. To develop a mechanistic understanding and a theory for trapping skinning, which occurs at higher drying-gas flow rates, non-Fickian drying behavior at low drying-gas flow rates is compared to that at high flow rates.

Figure 4 shows the predicted coating temperature and displays the three drying periods for a 100-micron dry-film thickness PMMA/acetone coating dried in an oven at 353 K and a heat-transfer coefficient of 209 (W/m^2/K). The drying behavior is investigated at points *A* (1 s) and *B* (10 s) in the warmup period, at points *C* (25 s) and *D* (75 s) in the constant-rate period, and at point *E* (150 s) in the falling-rate period. Nonisothermal non-Fickian drying behavior of the coating is investigated by analyzing concentration profiles; stress; Fickian flux, $D(dC/d\xi)$; and non-Fickian flux, $E(d\pi/d\xi)$, across the coating thickness at each of the points labeled in Figure 4.

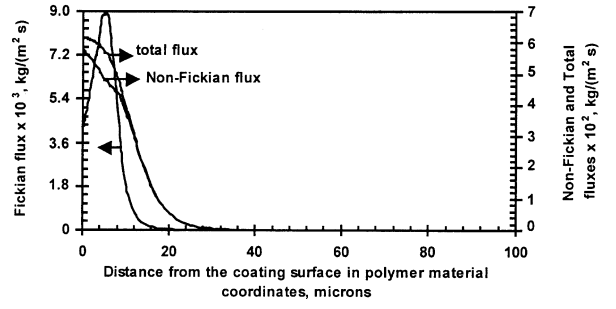

(b)

Figure 5b. Fickian flux, the non-Fickian flux, and the total flux profiles in the warmup period at 1 s at point *A*.

The Fickian flux exhibits a peak and the high non-Fickian flux causes flat concentration profile near the coating surface.

Drying behavior in the warmup period

Figure 5a shows solvent concentration and stress profiles after 1 s of drying time. The concentration profile shows a sigmoidal shape. Previous drying models based on Fick's law of diffusion with concentration-dependent diffusion coefficients did *not* predict a sigmoidal shape in the concentration profile. Fickian diffusion models predict a sharp decrease in the solvent concentration at the coating surface that corresponds to a drastic decrease in the diffusion coefficient at the coating surface. Therefore, the drop in the diffusion coefficient is balanced by a steep concentration gradient so that the internal solvent mass flux (at the coating surface, inside the coating) matches the external mass flux, which is determined by the mass-transfer coefficient and the solvent concentration at the surface. In contrast, the non-Fickian model predicts a *flat* concentration profile in a thin layer near the coating surface. The fall in the solvent concentration near the coating surface results in an increase in stress magnitude at the coating surface, which drives non-Fickian flux. The stress is zero initially and becomes negative with a fall in solvent concentration. The high non-Fickian flux (due to stress gradients) near the coating surface, shown in Figure 5b, acts like a pump, drawing more solvent to the coating surface, and flattens the solvent concentration profile near the coating surface.

If stress did not relax, then according to Eq. 5, the stress at the surface would be equal to the difference between the surface solvent concentration and initial concentration. Stress relaxation, however, causes the magnitude of stress near the coating surface to be considerably less than the change in solvent concentration. At 1 s values of relaxation time in the coating ranges from 1.12 s at the coating surface to 4.85×10^{-3} s at the substrate. Equation 5 indicates that the magnitude of stress at any node depends on two competing effects: the rate of change of the solvent concentration, that is, the strain rate, and the rate of relaxation (characterized by relaxation time) at the node. The strain rate dominates near the coating surface, and stresses develop at the surface, even though relaxation times are short.

Figure 5b shows Fickian flux (FF) and non-Fickian flux (NFF) through the coating thickness, and that the NFF dominates the solvent mass transport after 1 s. Figure 5b depicts a peak in the FF at a distance of approximately $\xi = 5$ microns from the coating surface. The peak does not correspond to maximum solvent concentration gradient inside the coating shown in Figure 5a. This is because the lower solvent concentration gradient $\xi = 5$ microns is compensated for by the higher mutual diffusion coefficient. Flat concentration gradients cause a decrease in the FF near the coating surface. There is a monotonic increase in the non-Fickian flux (NFF) from the substrate to the coating surface. Since stress gradients are steeper near the surface than those inside the coating, NFF is higher near the coating surface.

Due to the rapid heat transfer, the coating temperature rises to 328 K at 10 s (point *B*). Figure 6a shows that the solvent concentration profile retains a prominent sigmoidal

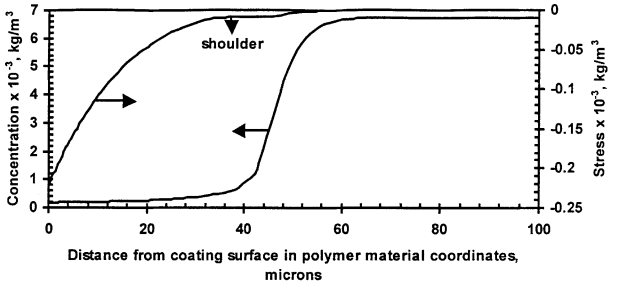

(a)

Figure 6a. Solvent concentration and stress profiles of 100-micron dry-film thickness poly(methyl methacrylate)/acetone coating at 10 s at point *B*.

Coating temperature is 328 K and the region of flat concentration profile is thicker than that at point *A*.

shape; the region of flat concentration near the coating surface is thicker than it is at point *A* and stress gradients are high throughout this region. Figure 6a demonstrates a relatively steep front in the solvent concentration, which moves into the coating. At points deeper than the front, π is approximately zero, but above the front, π develops and is negative. The NFF is higher in the thicker region at the coating surface mentioned earlier—higher at point *B* than it is at point *A*—due to stress development in this region of the coating. The higher NFF causes the flat concentration at the coating surface to grow bigger at point *B* than at point *A*. In this thick region, the FF and the NFF are nearly constant, because of the flat concentration gradients and almost constant stress gradients.

Figure 6a displays a shoulder in the stress profile, which indicates relaxation in the polymer. Shoulder formation is due to stress relaxation near the coating surface and stress development deeper within the coating. At the beginning of drying, due to high solvent concentrations, relaxation times are short and the stress relaxes near the coating surface. The stress develops deeper within the coating due to a decrease in the solvent concentration. The NFF in Figure 6b shows a dip and becomes negative due to stress relaxation in the

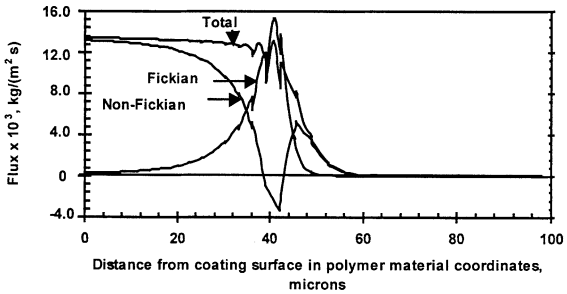

(b)

Figure 6b. Fickian flux, the non-Fickian flux, and the total flux profiles at 10 s at point *B*.

The peak in the Fickian flux occurs deeper than it did at point *A* and the non-Fickian flux becomes negative due to stress relaxation.

shoulder region of the stress profile. In Figure 6b, the wiggles in the NFF and the FF are due to the discontinuity of the basis functions at the element boundaries. The wiggles disappear when the number of elements is increased. In this article, however, we did not increase the number of elements, but used only 40 elements because doubling the number of elements changed the C and π values by at the most 0.5%.

The warmup period is marked by (1) development of the sigmoidal shape concentration profile, (2) stress relaxation inside the coating, (3) movement of the peak in the FF into the coating, and (4) a decrease in the NFF inside the coating. The sigmoidal shape concentration profile and the peak in the FF are two main features of the warmup period predicted by this model. Fickian models do *not* predict a flat concentration profile near the surface and the peak in the FF.

Drying behavior in the nearly constant-rate period

Figure 4 shows that the coating temperature at 25 s (point *C*) is 345 K approaching a shoulder in the temperature profile. Figure 7a shows that the solvent concentration profile remains nearly flat near the coating surface. Figure 7a also shows that the stress relaxes in the region from approximately 45 microns to 56 microns. The stress relaxation causes the NFF to vanish, and the FF stays constant in this region of the coating. Almost constant FF and vanishingly low NFF lead to a very low rate of change in the solvent concentration in this region. Figure 7a also shows that at nodes closer to the substrate, the solvent concentration starts decreasing and stresses develop. This leads to increase in the NFF and the FF, shown in Figure 7b, and the NFF decreases and becomes negative, while the FF increases and peaks closer to the substrate. The negative NFF occurs due to stress relaxation at the high coating temperature and the high solvent concentrations deeper in the coating. At the coating–substrate interface, stress does not develop, because the solvent concentration has not decreased from its initial value. As a result both the NFF and the FF are zero at the substrate.

At 75 s (point *D*), the coating is almost at the end of the nearly constant-rate period and the coating temperature is 349 K, which is close to the drying-gas temperature of 353 K. Figure 8a shows the development of a steep concentration gradient near the coating surface. The solvent concentration gradient becomes steep at the coating surface so that the internal solvent mass flux matches the external flux, which is high due to the high mass-transfer coefficient at high drying-gas flow rate. Figure 8b shows that the NFF becomes negative at approximately $\xi = 32$ microns. This is due to the stress relaxation inside the coating that occurs due to the short relaxation times at the high coating temperature. The negative NFF also causes a steep solvent concentration gradient inside the coating, shown in Figure 8a, which results in a peak in FF.

At the beginning of the nearly constant-rate period, a layer of zero NFF and constant FF develops inside the coating. This layer grows in thickness with time toward the substrate. During this period the stress relaxes near the substrate and causes a negative peak in the NFF. The NFF also becomes negative near the coating surface due to stress relaxation during the end of this period. This results in a solvent front near

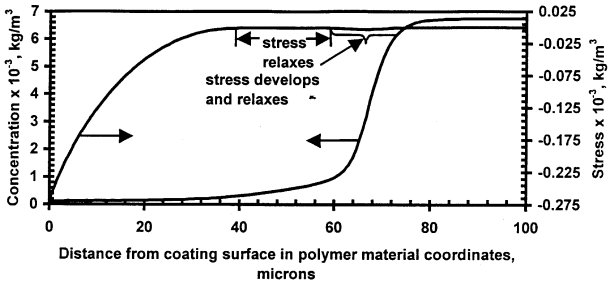

(a)

Figure 7a. Solvent concentration and stress profiles of 100-micron dry-film thickness poly(methyl methacrylate)/acetone coating at the beginning of the nearly constant-rate period at 25 s at point *C*.

Coating temperature is 345 K; Stress develops near the substrate while it relaxes in the middle of the coating.

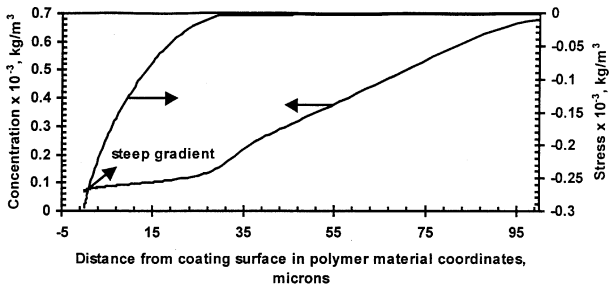

(a)

Figure 8a. Solvent concentration and stress profiles of 100-micron dry-film thickness poly(methyl methacrylate)/acetone coating at the end of the nearly constant-rate period at 75 s at point *D*.

Coating temperature is 349 K; Steep concentration gradient begins to form near the coating surface.

the coating surface. A steep solvent concentration gradient also forms near the coating surface to match the internal solvent flux with the external flux.

Drying behavior in the falling-rate period

In the falling-rate period, the drying rate becomes low due to low diffusion coefficients. Therefore, the heat consumption due to solvent evaporation decreases and the coating temperature rises and reaches the drying-gas temperature. Also, due to low diffusion coefficients the solvent concentration decreases very slowly throughout the coating in this period.

Figure 9a shows that after 150 s of drying, the solvent concentration at point E is low in the thin surface layer, shown by the solid line, near the coating surface and higher inside in the thick layer near the substrate, depicted by the dotted line. Near the shoulder region of the stress profile, the NFF becomes negative (shown in Figure 9b). This negative NFF causes a steep solvent concentration gradient near the coating surface. The NFF remains negative for the remaining drying period, because the stress does not relax significantly anywhere in the coating, due to very high relaxation times that range from 6.57×10^{8} s at the coating surface to 6.24×10^{3} s at the substrate. The magnitude of the stress inside the coating increases very slowly due to the very slow decrease in the solvent concentration. Thus, the stress profile maintains its shape for the remaining drying period due to the slow decrease in the solvent concentration and high relaxation times.

The drying behavior in the falling-rate period is marked by the development of a thin layer of low solvent concentration near the coating surface and a thick layer of higher solvent concentration inside the coating. The negative NFF causes a steep solvent concentration gradient inside the coating. The stress does not relax and the NFF remains negative in a narrow region near the coating surface for the remainder of the drying period.

Process Paths

Process paths display the concentration, the stress, and the coating temperature at any node during drying. Figures 10, 11a and 11b show the process paths traversed by several nodes

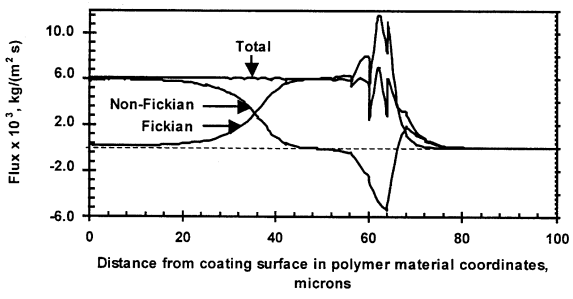

(b)

Figure 7b. Fickian flux, the non-Fickian flux, and the total flux profiles at the beginning of the nearly constant-rate period at 25 s at point *C*.

A region of zero non-Fickian and constant Fickian flux develops inside the coating.

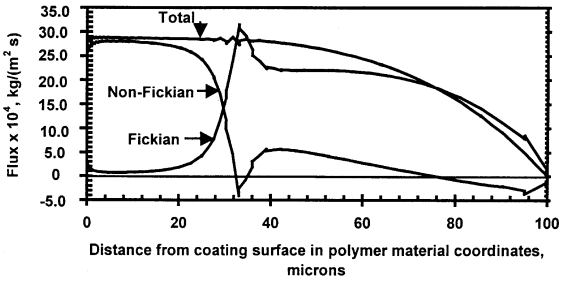

(b)

Figure 8b. Fickian flux, the non-Fickian flux, and the total flux profiles at the end of the nearly constant-rate period at 75 s at point *D*.

The non-Fickian flux becomes negative near the coating surface and near the substrate due to stress relaxation.

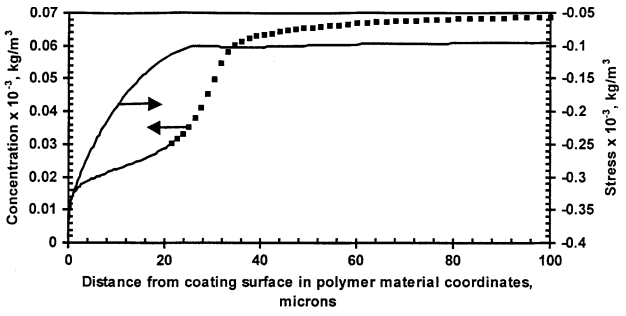

(a)

Figure 9a. Solvent concentration and stress profiles of 100-micron dry-film thickness poly(methyl methacrylate)/acetone coating in the falling-rate period at 150 s at point *E*.

Coating temperature is 349 K. The solid line shows region of low solvent concentration at the coating surface, and the dotted line shows region of high solvent concentration inside the coating.

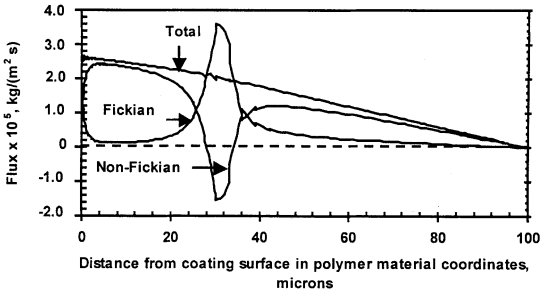

(b)

Figure 9b. Fickian flux, the non-Fickian flux, and the total flux profiles in the falling-rate period at 150 s at point *E*.

The non-Fickian flux becomes negative near the coating surface due to stress relaxation.

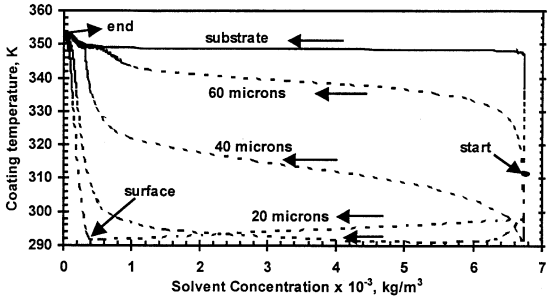

Figure 10. Solvent concentration at various locations in the coating and the coating temperature for a 100-micron dry-polymer thickness poly(methyl methacrylate)/acetone coating at a drying gas temperature of 353 K and a heat transfer coefficient of 209 (W/m^2/K).

The dotted line, the serrated line and the thick line indicate the warmup, the nearly constant rate and the falling rate periods respectively.

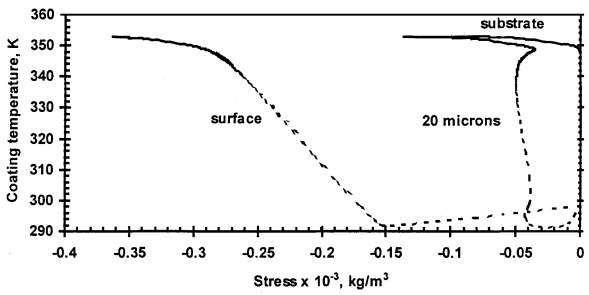

(a)

Figure 11a. Stress at the surface, at a distance of 20 microns into the coating from the surface and at the substrate and the coating temperature for a 100-micron dry-polymer thickness poly(methyl methacrylate)/acetone coating at a drying-gas temperature of 353 K and a heat-transfer coefficient of 209 (W/m^2/K).

The dotted line, the serrated line, and the thick line indicate the warmup, the nearly constant-rate, and the falling rate periods, respectively.

at different distances from the coating surface in the three drying periods at a heat-transfer coefficient of 209 (W/m^2/K) and a drying-gas temperature of 353 K. The dotted line, the serrated line, and the thick solid line in these figures indicate the warmup, the nearly constant-rate, and the falling-rate periods, respectively.

Warmup period

Figure 10 shows that the solvent concentration at the coating surface drops rapidly in the warmup period with a small drop in coating temperature due to evaporative cooling. Fig-

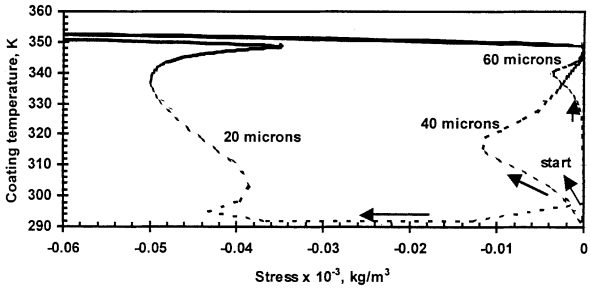

(b)

Figure 11b. Stress at various locations in the coating and the coating temperature for a 100-micron dry-polymer thickness poly(methyl methacrylate)/acetone coating at a drying-gas temperature of 353 K and a heat-transfer coefficient of 209 (W/m^2/K).

The dotted line, the serrated line, and the thick line indicate the warmup, the nearly constant-rate, and the falling-rate periods, respectively.

ure 11a shows that the magnitude of the surface stress increases, which is due to a sudden decrease in surface solvent concentration. Due to the rapid heat transfer from the drying gas, the coating temperature rises rapidly and the surface solvent concentration drops further with a concomitant increase in surface stress, as shown in Figure 11a. During this period, the stress relaxes slightly at the surface because the effect of the rate of decrease in the surface solvent concentration overrides the effect of relaxation at the beginning. Relaxation times are high due to lower solvent concentrations at the end of this period and the stress at the surface does not relax.

Figure 10 shows that at the substrate the solvent concentration does not change from its initial value in the warmup period. Therefore, during the warmup period, the stress does not develop at the substrate, as shown in Figure 11a. Figure 10 indicates that the change in the solvent concentration from its initial value decreases more slowly at nodes deeper in the coating. Therefore, the relaxation times are shorter at these nodes, due to higher solvent concentrations, and the stress relaxes significantly, as shown in Figure 11b. The stress relaxation deeper in the coating causes negative stress gradients during the end of the warmup period. This causes negative NFF, as shown in Figure 6b.

Nearly constant-rate period

Figure 10 shows that the solvent concentration at all the locations continues to decrease in the nearly constant-rate period because of high transport coefficients due to the high coating temperature. Figure 11a shows that the stress does not relax at the coating surface. Even though the coating temperature is high, the relaxation times are high at the coating surface because of low solvent concentrations. Figure 11b shows that during this period, the stress relaxes considerably at the nodes 20%, 40%, and 60% in the coating, because of low relaxation times at high coating temperatures. The stress relaxation causes negative NFF, as shown in Figures 7b and 8b.

Falling-rate period

Figure 10 shows that the coating temperature approaches the drying-gas temperature and that the solvent concentrations are low and decrease at all the locations. Due to low solvent concentrations, the relaxation times are very high and the stress increases slowly at all three points, as shown in Figures 11a and 11b. Since the solvent concentration decreases and the stress magnitude increases, both slowly, the drying behavior does not change qualitatively in this period.

Anomalous Trapping-Skinning Behavior

Trapping skinning occurs when *more* solvent remains inside the coating that is dried at *higher* drying-gas flow rate and/or temperature. Trapping-skinning behavior is anomalous because, as explained in the Introduction, Fick's law of diffusion with concentration-dependent diffusion coefficients cannot explain it. So, this work attempts to find an explanation for trapping skinning by investigating non-Fickian drying behavior of the polymer coatings.

Figure 12 shows the residual solvent content at low and high heat-transfer coefficients [20.9 and 209 ($W/m^2/K$] that correspond to low and high drying-gas flow rates at a drying-gas temperature of 353 K for a 100-micron dry-film thickness PMMA/acetone coating. Residual solvent content at the higher drying-gas flow rate initially decreases faster than that at low gas flow rate. But eventually, Figure 12 shows a crossover, and the residual solvent content is *more* at *higher* drying gas flow rates. This crossover depicts the fundamental characteristic feature of trapping-skinning behavior of the polymer coatings and is in keeping with the arguments proposed by Edwards (1998).

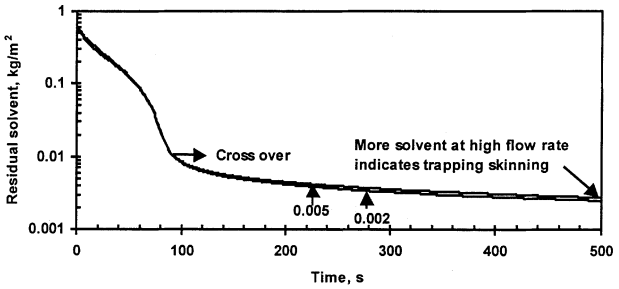

Figure 12. Residual solvent at two different heat-transfer coefficients (or different drying gas flow rates) for a 100-micron-thickness poly-(methyl methacrylate)/acetone coating at 353 K drying-gas temperature.

The cross over that occurs at approximately 310 s indicates trapping skinning.

DASSL integrates the residual equations until the norm of the residuals converges to 10^{-6}. The residual solvent is computed from Eq. 9, which integrates the solvent concentration through the film. At 500 s, the solvent concentration varies from 4.14×10^{-4} at the surface to 3.75×10^{-2} at the substrate. The contribution to residual solvent due to elements deeper in the coating becomes progressively higher because of a higher solvent concentration and larger elements. Hence, our results are not comparable to error, and the increase in residual solvent at higher gas flow rate appears small because we chose the logarithmic scale for the *y*-axis.

The explanation for trapping skinning is as follows. At a lower drying-gas flow rate, the coating temperature rises slowly to the drying-gas temperature due to lower heat-transfer rate, as shown in Figure 13a. Due to this slow rise in the coating temperature, in the warmup period, stress relaxation occurs deeper within the coating because of high solvent concentrations. Consequently, the minimum in NFF, in the warmup period, occurs deeper within the coating at a low flow rate than it does at a high flow rate. In the nearly constant-rate period, the negative NFF near the coating surface occurs deeper at lower gas flow rates. Figure 13b shows that in the falling-rate period, the NFF stays negative deeper within the coating at lower drying-gas flow rates. This persistent negative NFF causes a steep solvent concentration gradient deeper in the coating at a lower drying-gas flow rate. Figure 14 compares the solvent concentration profiles at 500 s at two different flow rates (or heat-transfer coefficients) at a drying-gas temperature of 353 K. The solid and dotted lines in Figure 14 indicate regions near the coating surface and deeper within the coating, respectively. At lower drying-gas

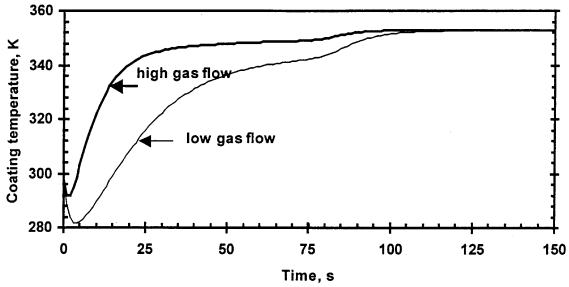

(a)

Figure 13a. Coating temperature evolution for a 100-micron-thickness poly(methyl methacrylate)/acetone coating at 353 K drying-gas temperature at low and high gas flow rates.

The coating temperature rises faster at higher gas flow rate.

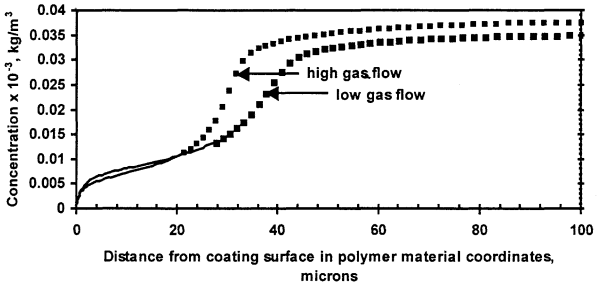

Figure 14. Solvent concentration profiles at 500 s for two different heat-transfer coefficients (or different drying-gas flow rates) for a 100-micron-thickness poly(methyl methacrylate)/acetone coating at 353 K drying-gas temperature.

Drying at higher flow rates leads to thinner region of low solvent concentration and thicker region of high solvent concentration inside the coating.

flow rates, the negative NFF, and, therefore, the steep concentration gradient, occur deeper within the coating. Hence, the region of the low solvent concentration near the coating surface is thicker, and the region of high solvent concentration is thinner at low drying-gas flow rates, as shown in Figure 14.

At a higher drying gas flow rate, the coating temperature rises faster until it reaches the drying-gas temperature. Therefore, in the nearly constant-rate period, the stress relaxes closer to the coating surface. Consequently, the NFF becomes negative near the coating surface during the nearly constant-rate period. The stress does not relax anywhere in the coating due to the high relaxation times in the falling-rate period. Hence, the NFF remains negative and results in the development of a thinner layer of low solvent concentration near the surface and a thicker layer of high solvent concentration deeper within the coating. Thus, the residual solvent content is higher in the coatings dried at higher drying-gas flow rates. The higher residual solvent content at the higher drying-gas flow rate is the essence of trapping-skinning behavior of the polymer coatings.

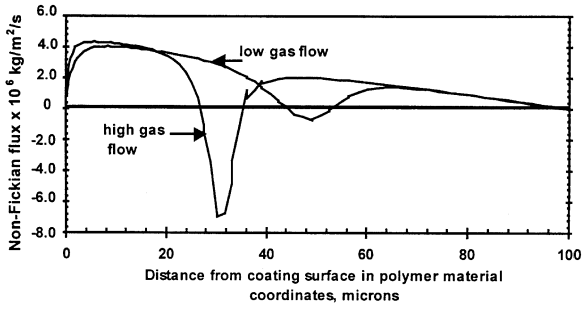

(b)

Figure 13b. Non-Fickian flux profile at 500 s at low and high flow rates for a 100-micron-thickness poly(methyl methacrylate)/acetone coating at 353 K drying-gas temperature.

The non-Fickian flux becomes negative closer to the coating surface at higher gas flow rates.

Figure 15 shows that the residual solvent content decreases monotonically with the drying-gas temperature at several different drying-gas flow rates, which are represented by different heat-transfer coefficients. Although trapping skinning occurs at higher flow rates at the same drying gas temperature, it does not occur at higher drying-gas temperatures for the same flow rate. Stress relaxation occurs closer to the surface at higher drying-gas temperatures. Therefore, the NFF becomes negative closer to the coating surface than it does at lower temperatures. As a result, the solvent concentration gradient becomes steeper closer to the coating surface at higher temperatures. The region of low solvent concentration near the coating surface gets thinner at higher temperatures. But this does not lead to trapping skinning, because at higher temperatures, the solvent concentration is lower both near the coating surface and deeper within the coating than it is at lower temperatures, due to higher transport coefficients.

Figure 16 compares experimentally measured residual acetone with that predicted by the model for 15-micron-thick poly(methyl methacrylate)/acetone coatings at a drying-gas temperature of 323 K at different gas velocities. Table 3 gives the heat- and mass-transfer coefficients corresponding to the gas velocities in Figure 16. The model predictions capture the trend in the variation of the residual acetone with the drying-gas flow rate. There is, however, a significant difference between the experimental results and the model predictions. The model presented in this article contains several parameters that are adjustable, as discussed in the Model Parameters section. In our model predictions, we have adjusted the diffusion parameters and used a value of 3.0×10^{-4} and -370.0 for the preexponential factor, D_o, and the polymer free volume parameter, $K_{22} - T_{g2}$, respectively. A regression analysis, which is beyond the scope of this article, can be used to obtain sets of adjustable parameters that minimize experimental-model mismatch.

Conclusions

As the solvent leaves the coating surface during drying, stress develops due to coating shrinkage. The diffusion Debo-

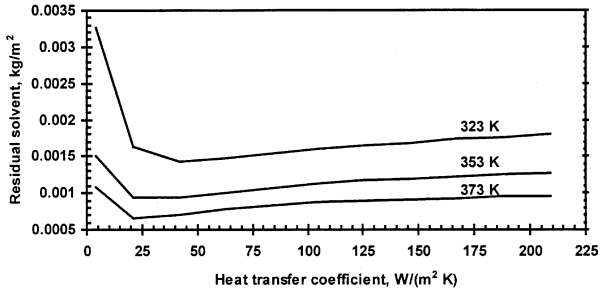

Figure 15. Residual solvent content at three drying-gas temperatures and several different heat-transfer coefficients (or different drying-gas flow rates) for a 100-micron-thickness poly(methyl methacrylate)/acetone coating.

Residual solvent content shows a minimum with gas flow rate and decreases monotonically with drying-gas temperature.

rah number (De) characterizes the relaxation and diffusion times, and indicates whether significant stresses will develop. For PMMA/acetone solutions, De is $O(1)$ at low mass fractions of acetone, and, therefore, stress contributes to solvent transport. This work describes the drying behavior of the PMMA/acetone coatings by a non-Fickian, nonisothermal model by investigating the concentration, stress, Fickian flux (FF), and non-Fickian flux (NFF) profiles during the warmup, nearly constant-rate, and falling-rate periods.

The drying behavior in the warmup period is marked by a sigmoidal shape concentration profile due to the high NFF

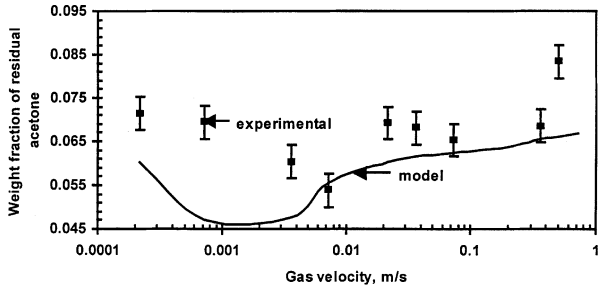

Figure 16. Experimental and model predictions of weight fraction of residual acetone for a 15-micron dry-film thick poly(methyl methacrylate)/acetone coating at a drying-gas temperature of 323 K.

The initial weight fraction of acetone is 95%. The model captures the trend in variation of residual acetone with gas velocity.

near the coating surface. Stress that develops due to shrinkage of the coating relaxes near the substrate during this period. The FF exhibits a peak that moves into the coating and the NFF develops a dip inside the coating that is due to stress relaxation.

The solvent concentration profile becomes steep near the coating surface during the end of the nearly constant-rate period. A zero NFF and a constant FF region develops near the substrate due to stress relaxation. The thickness of this region grows with time toward the substrate. In the falling-rate period, the coating temperature rises to the drying-gas temperature. Relaxation times are very high across the coating thickness because of low solvent concentrations. Therefore, stress does not relax, but increases slowly due to the slow decrease in the solvent concentration. The NFF becomes and stays negative near the coating surface, leading to a thin region of low solvent concentration near the coating surface and a thick region of high solvent concentration inside the coating.

The model presented in this work predicts trapping skinning, an anomalous drying behavior of polymer coatings, at higher drying gas flow rates and suggests a plausiable explanation for it. Due to stress relaxation closer to the surface, the region of low solvent concentration near the coating surface is thinner and the region of high solvent concentration becomes thicker at higher drying-gas flow rates. Hence, trapping skinning occurs at higher drying-gas flow rates. At higher drying-gas temperatures, stress relaxes closer to the surface than it does at lower gas temperature. Stress relaxation causes the formation of a thicker region of high solvent concentration deeper within the coating and a thinner region of low solvent concentration closer to the surface. But, the total residual solvent content is still lower at higher drying gas temperatures, because the solvent levels in both regions are lower due to high transport coefficients at higher temperatures. Hence, trapping skinning does not occur at higher drying-gas temperatures.

The model results on trapping skinning at higher flow rates match qualitatively with our experimental measurements for PMMA/Ac coatings. The model parameters, such as polymer free volume parameters, preexponential factor, D_o, and the molar ratio of the solvent jumping unit to polymer jumping unit, are usually unknown and need to be estimated through experiments at high temperatures, where non-Fickian transport is negligible. Also, the reference relaxation time and the shear modulus of the pure polymer should be accurately estimated. We believe that if De becomes $O(1)$ during drying, the polymer coating may exhibit trapping-skinning behavior at higher drying gas flow rates.

The non-Fickian model helps choose appropriate operating conditions, such as drying-gas flow rate and temperature,

Table 3. Heat-Transfer Coefficients and Mass-Transfer Coefficients Estimated from Experiments on HADES and Corresponding Residual Weight Fraction of Acetone (Vinjamur and Cairncross, 2002)

HTC (W/m^2/K)	0.383	0.803	1.79	2.55	4.40	5.68	8.03	17.9	21.3
MTC $\times$ 10^5 (kg/m^2/s/Pa)	0.12	0.21	0.48	0.67	1.17	1.5	2.13	4.73	5.53
Weight fraction ($\times 10^2$) with adjustment	6.04	4.72	4.76	5.55	6.04	6.16	6.24	6.40	6.56
Weight fraction $\times$ 10^2) from experiment	7.14	6.94	6.03	5.38	6.92	6.81	6.53	6.85	8.33

to meet residual solvent specifications. The model can also be used to predict bubble formation that can occur at higher drying-gas temperatures and at higher flow rates due to rapid heat transfer. This will help in developing drying regimes that identify the operating conditions where skinning and bubbles occur. These regimes can be used to design and operate the dryers to produce defect-free polymer coatings.

Acknowledgments

We gratefully acknowledge the financial support from 3M and Avery Dennison.

Literature Cited

Alfrey, T., E. F. Gurnee, and W. G. Lloyd, "Diffusion in Glassy Polymers," *J. Poly. Sci. Part C*, **12**, 249 (1996).

Alsoy, S., and J. L. Duda, "Drying of Solvent Coated Polymer Films," *Drying Technol.*, **16**(1&2), 15 (1998).

Alsoy, S., and J. L. Duda, "Modeling of Multicomponent Drying of Polymer Films," *AIChE J.*, **45**, 896 (1999).

Barr-Howell, B. D., and E. J. Gordon, "A Study of the Transport Properties of Solvent Desorption from Experimental Films Using Thermogravimetric Analysis," *Thermochem. Acta*, **180**, 147 (1991).

Beris, A. N., and B. J. Edwards, *Thermodynamics of Flowing Systems*, Oxford, New York (1994).

Billovits, G. F., and C. J. Durning, "Polymer Material Coordinates for Mutual Diffusion in Polymer Penetrant Systems," *Chem. Eng. Commun.*, **82**, 21 (1989).

Billovits, G. F., and C. J. Durning, "Linear Viscoelastic Diffusion in the Poly(styrene)-Ethylbenzene System: Comparison Between Theory and Experiment," *Macromolecules*, **27**, 7630 (1994).

Brenan, K. E., S. L. Campbell, and L. R. Petzold, *Numerical Solution of Initial-Value Problems in Differential-Algebraic Equations*, Elsevier, New York (1989).

Cairncross, R. A., "Solidification Phenomena During Drying of Sol-to-Gel Coatings," PhD Thesis, Univ. of Minnesota, Minneapolis (1994).

Cairncross, R. A., and C. J. Durning, "A Model for Drying of Viscoelastic Polymer Coatings," *AIChE J.*, **42**, 2415 (1996).

Carbonell, R. G., and G. C. Sarti, "Coupled Deformation and Mass Transfer Processes in Solid Polymers," *Ind. Eng. Chem. Res.*, **29**, 1194 (1990).

Chow, T. S., "Molecular Interpretation of the Glass Transition Temperature of Polymer-Diluent Systems," *Macromolecules*, **13**, 362 (1980).

Crank, J., "The Influence of Concentration Dependent Diffusion Coefficient on Rate of Evaporation," *Trans. Faraday Soc.*, **46**, 450 (1950).

Crank, J., "Diffusion in Polymers: Some Anomalies and Their Significance," *Trans. of Faraday Soc.*, **47**, 1072 (1951).

Duda, J. L., and Vrentas, J. S., "Mathematical Analysis of Sorption Experiments," *AIChE J.*, **17**, 464 (1971).

Durning, C. J., "Differential Sorption in Viscoelastic Fluids," *J. Poly. Sci., Poly. Phys. Ed.*, **23**, 1831 (1985).

Durning, C. J., and M. Tabor, "Mutual Diffusion in Concentrated Polymer Solutions Under a Small Driving Force," *Macromolecules*, **19**, 2220 (1986).

Edwards, D. A., "Theoretical Predictions of Trapping Skinning," *Chem. Eng. Commun.*, **166**, 201 (1998).

Ferry, J. D., *Viscoelastic Properties of Polymers*, Wiley, New York (1980).

Finlayson, B. A., *Numerical Methods of Problems with Moving Fronts*, Ravenna Park Publishers, Seattle, WA (1992).

Flory, P. J., *Principles of Polymer Chemistry*, Cornell Univ. Press, Ithaca, NY (1953).

Fuchs, K., C. Friedrich, and J. Weese, "Viscoelastic Properties of Narrow Distribution of Poly(methyl methacrylates)," *Macromolecules*, **29**, 5893 (1996).

Gutoff, E., "Modeling the Drying of Solvent Coatings on Continuous Webs," *J. Imaging Sci. Technol.*, **38**, 184 (1994).

Hassan, M. M., and C. J. Durning, "Effects of Polymer Molecular Weight and Temperature on Case II Transport," *J. Poly. Sci., Poly. Phys. Ed.*, **37**, 3159 (1999).

Hong, S., "Prediction of Polymer/Solvent Diffusion Behavior Using Free Volume Theory," *Ind. Eng. Chem. Res.*, **34**, 2536 (1995).

Jou, D., J. Casas-Vazquez, and G. Lebon, *Extended Irreversible Thermodynamics*, Springer-Verlag, New York (1993).

Lustig, S. R., J. M. Ceruthers, and N. A. Peppas, "Continuum Thermodynamics and Transport Theory for Polymer-Fluid Mixtures," *Chem. Eng. Sci.*, **47**, 3037 (1992).

Neogi, P., "Anomalous Diffusion of Vapors through Solid Polymers: I. Irreversible Thermodynamics of Diffusion and Solution Processes," *AIChE J.*, **29**, 829 (1983).

Okazaki, M., K. Shioda, K. Masada, and R. Toei, "Drying Mechanism of Coated Film of Polymer Solution," *J. Chem. Eng. Jpn.*, **7**, 99 (1974).

Peterlin, "Diffusion in a Network with Discontinuous Swelling," *J. Poly. Sci., Poly. Lett.*, **3**, 1083 (1965).

Petzold, L. R., "A Description of DASSL: A Differential Algebraic System Solver,"Sandia National Laboratories Rep., SAND 82-8637, available at http://infoserve.sandia. gov/sand − doc/1982/828637.pdf (1982).

Price, P. E., S. Wang, and I. Hadj Romdhane, "Extracting Effective Diffusion Parameters from Drying Experiments," *AIChE J.*, **43**, 1925 (1997).

Romdhane, I. H., P. E. Price, C. A. Miller, P. T. Benson, and S. Wang, "Drying of Glassy Polymer Films," *Ind. Eng. Chem. Res.*, **40**(14), 3065 (2001).

Strang, G., and G. J. Fix, *An Analysis of the Finite Element Method*, Prentice Hall, Englewood Cliffs, NJ (1973).

Thomas, N. L., and A. H. Windle, "Transport of Methanol in Poly(methyl methacrylate)," *Polymer*, **19**, 255 (1978).

Thomas, N. L., and A. H. Windle, "A Theory of Case II Diffusion," *Polymer*, **23**, 529 (1982).

Vinjamur, M., and R. A. Cairncross, "Experimental Investigations of Trapping Skinning," *J. Appl. Poly. Sci.*, **83**, 2269 (2002).

Vrentas, J. S., and J. L. Duda, "Diffusion in Polymer Solvent Systems," *J. Poly. Sci., Polym. Phys. Ed.*, **15**, 403 (1977).

Vrentas, J. S., and C. M. Vrentas, "Drying of Solvent Coated Polymer Films," *J. Poly. Sci., Poly. Phys. Ed.*, **32**, 187 (1994).

Vrentas, J. S., C. M. Jarzebski, and J. L. Duda, "A Deborah Number for Diffusion in Polymer Solvent Systems," *AIChE J.*, **21**, 894 (1975).

Wang, B., T. Yamaguchi, and S. Nakao, "Solvent Diffusion in Amorphous Glassy Polymers," *J. Poly. Sci., Poly. Phys. Ed.*, **38**, 846 (2000).

Wagner, G. R., E. U. Schlunder, and R. Saure, "Drying of Solvent Borne Polymeric Coatings: Modeling the Drying Process," *Surf. Coating Technol.*, **99**, 253 (1998).

Yapel, R. A., "A Physical Model of the Drying of Coated Films," MS Thesis, Univ. of Minnesota, Minneapolis (1988).

Manuscript received July 13, 2001, and revision received Apr. 26, 2002.